

# Prediction of Maximum Yield in the Crystallization of Multicomponent Isomeric Systems

Alan A. Smith,<sup>\*,†</sup> Ben McKay, Eric W. P. Damen,<sup>‡</sup> Simone Darphorn-Hooijschuur, Erik-Jan Ras, and Goran Verspui<sup>‡</sup>  
*Avantium Technologies BV, Zekeringstraat 29 1014 BV, The Netherlands*

## Abstract:

We have developed a computer program (CRYSS), which may be used to rank the performance of a series of crystallization experiments. The method, at its simplest, allows the chemist to take composition data from partially purified crystallized solids and mother liquors; when this is coupled with initial composition data, the program can predict the maximum yield the system is capable of delivering after optimization. In this paper the underlying theoretical basis of the method is investigated by means of the crystallization of a three-component blend of hydrobenzoin isomers, along with the investigation of a four-component system based on aminoindanol. In the latter case, the modulation of purification performance via salt formation is demonstrated.

## Introduction

We are well aware that chemical reactions result in crude product, which contains the desired component along with a mixture of unwanted compounds. Often these are structurally similar to the desired product, which can make crystallization-mediated separation challenging.

The development of parallel reactor systems and solid-/liquid-handling robots provide the chemist with the ability to conduct many more experiments than is possible manually. For the optimization of reaction work-up and product purification, these tools hold promise. In conducting a crystallization study comprising different solvents and/or salt formers under various crystallization conditions, one may end up with a large number of partially purified samples, along with some high-purity, low-yield samples. If one is fortunate enough to find a high-yielding, high-purity system and the economics are acceptable, then the problem is solved. If not, however, the challenge is then to identify the best systems in an array of partially optimized crystallizations!

The key issue which faces anyone attempting this type of investigation is the utilization of an efficient data processing routine. That is, a way of converting experimental data into knowledge and a means of getting more information out of fewer experiments. Without such a rational approach, using high throughput tools would add little.

We have developed a methodology for the rapid identification of crystallization systems capable of delivering high

yields. Moreover, ranking is possible when partial purification has been obtained, in principle, from a single experiment. The method involves using a numerical optimizer to fit parameters to a mechanistic model; the input data at its simplest is (i) composition data from the partially purified crystallized solid, (ii) mother liquor compositional analysis, and (iii) the starting composition.

**Conglomerate Enantiomer Mixtures.** Consider the simple case of a pair of enantiomers behaving as a conglomerate. These have identical melting points and heats of fusion and the same molecular architecture, differing only in that they are mirror images. A eutectic exists and is of a 50:50 composition. This is true, irrespective of the choice of solvent. This fact makes it relatively straightforward to purify an enantiomerically enriched mixture (i.e. one which may result from an asymmetric synthesis). To illustrate, let us assume that 100 g of a 90:10 mixture of enantiomers has been obtained, with the desired isomer being the major component. The maximum possible yield of pure enantiomer ( $R_{\max}$ ) corresponds to a solution of 10 g of the minor isomer, along with an equal portion (due to the 50:50 eutectic) of the desired isomer (i.e., 10 g). Complete removal of the unwanted isomer is achieved by dissolution of 20 g of material of 50:50 composition, providing 80 g of pure enantiomer. Thus, 80% ee gives 80% yield.

**Diastereomeric Mixtures.** Classical resolution consists of making a derivative of a racemic mixture (usually a salt) by application of a resolving agent. The beauty of this approach is two-fold: (i) the access to a wide range of resolving agents,<sup>1</sup> and (ii) the type of processes which result from this type of development work are usually applicable to general purpose batch reactor equipment.

The  $R_{\max}$  may be calculated using eq 1, where  $x_0$  is the initial composition (0.5 for a racemate),  $x_{\text{eu}}$  is the composition of the eutectic (in the range  $0 \leq 0.5$ ).

$$R_{\max} = \frac{(x_0 - x_{\text{eu}})}{(1 - x_{\text{eu}})} \quad (1)$$

This information is often expressed on the melting point phase diagram (Figure 1). It implicitly assumes ideal behaviour (in that changing the solvent will not change the composition of the binary eutectic).

This does not mean that the salts have the *same solubility* in all solvents but that their solubility ratio does not change significantly when switching solvents. Given that stereois-

\* To whom correspondence should be addressed. Telephone: +44 1263 822741. E-mail: alan.smith@lanxess.com.

<sup>†</sup> Current address: Lanxess Ltd., Strawberry Hill, Newbury, Berkshire RG14 1JA, UK

<sup>‡</sup> Current address: MercaChem Process Research BV, Kerkebos 1013, 6546 BB Nijmegen, The Netherlands

(1) Kozma, D. *CRC Handbook of Optical Resolutions via Diastereomeric Salt Formation*; CRC Press: Boca Raton, FL, 2002.

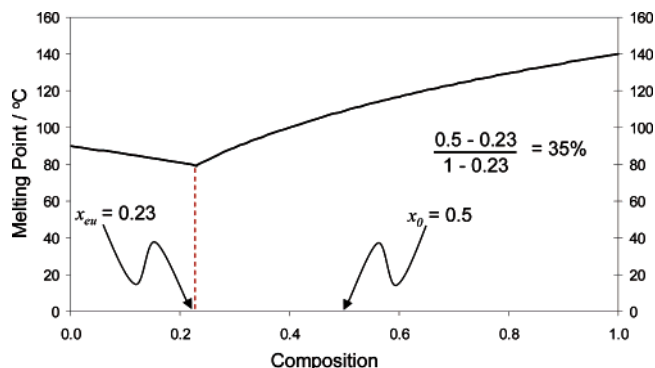


**Figure 1.** Typical melting point phase diagram of a diastereomer mixture.

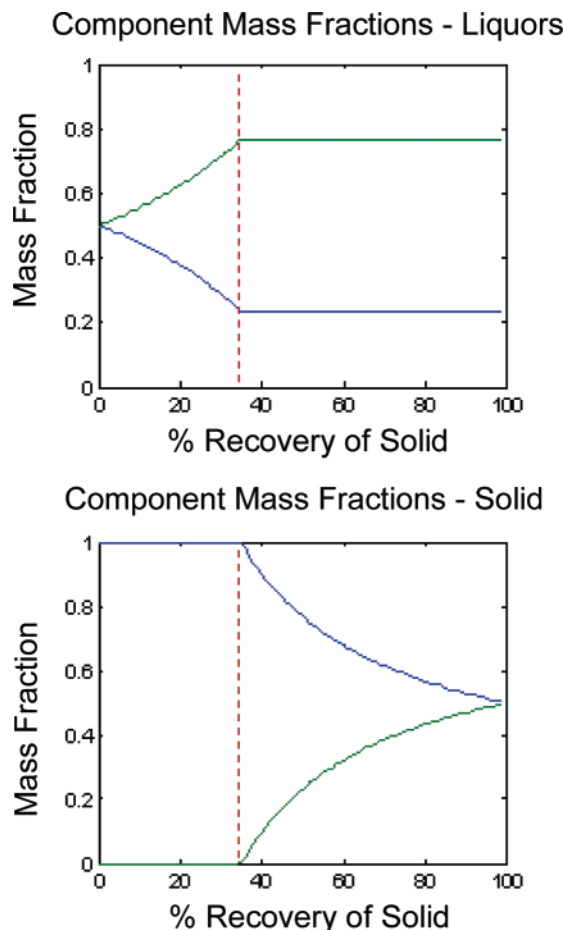


**Figure 2.** Purity profile for the solid and mother liquor phase of binary diastereomeric mixture as a function of mass fraction crystallized. The location of the red line denotes the maximum theoretical yield ( $R_{\max}$ ) of pure solid from the crystallization.

mers have the same functional groups and connecting framework, differing only in their arrangement in space and in the absence of strong conformational bias leading to differential solvent interactions or supramolecular interactions, discrimination of the stereoisomers by solvent may well be minimal.<sup>2</sup>

Figure 2 shows the profile of the crystallization of an ideal binary mixture of diastereomers, specified as a function of mass fraction crystallized. The upper chart relates to com-

position in the mother liquors, the lower describes the composition of the crystallized solid.

In the region just to the left of the red line, one obtains crystals of pure (blue) diastereomer. If more solvent is used in the crystallization, one will obtain the lower yield of pure diastereomer. If just the right amount of solvent is used, one obtains the maximum possible yield (35% in this case). If the amount of solvent used is reduced further, higher yields of increasingly impure material are obtained. Interestingly, from an investigative perspective, this is an attractive situation because the mother liquors now have eutectic composition and from eq 1 we know how to calculate  $R_{\max}$ .

**Multicomponent Mixtures (MultXeu).** In recent years there have been some interesting approaches in the field of diastereomer-mediated resolutions. These approaches make use of thermal analysis to determine the composition of the binary eutectic, which can be used to calculate the maximum yield ( $R_{\max}$ ) of the resolution.<sup>3</sup> When one has more than two components in a mixture, the situation is far more complex. Specifically, when partially purified material has crystallized, the mother liquors no longer have the eutectic composition. It is therefore not possible to readily calculate  $R_{\max}$ .

A mechanistic model for ideal multicomponent crystallizations has been described,<sup>4</sup> wherein a method for the calculation of  $n$ -dimensional eutectics was set out. It was also shown that the  $n$ -dimensional eutectic will be more soluble than the  $(n - 1)$ -dimensional eutectic, and consequently purification may be calculated through a series of steps. The overall recovery ( $R_{\max}$ ) is the product of the recoveries at each discrete purification step.

Unfortunately, the practicality of this model is limited since it requires melting point and heat of fusion data for all of the pure components. Also, since it is ideal, it neglects the effect of solvent and other interactions among the components.<sup>5</sup> Nevertheless, it did provide a framework for the understanding of multicomponent crystallizations.

In this paper a calculation using this ideal model is referred to as MultXeu. In order to obtain a MultXeu  $R_{\max}$  value, one requires (i) the initial composition of a mixture, (ii) the melting point and heat of fusion of the pure components and thermal data associated with racemic compounds where applicable, (iii) characterization of either conglomerate or racemic compound behaviour for the enantiomorphs, (iv) a computer program based on the published algorithm.

**CRYSS Model.** We have developed a system (referred to as CRYSS: CRYstallization Screening System) for analysing partially purified mixtures and predicting the maximum possible yield of the pure component ( $R_{\max}$ ). CRYSS is a predicative model based upon the measurement of the *actual system* at some arbitrary point during purification and the subsequent fitting of the model parameters to map the observed compositions.

- (3) (a) Kozma, D.; Pokol, G.; Ács, M. *J. Chem. Soc. Perkin Trans.* **1992**, 2, 435. (b) Madarász, J.; Kozma, D.; Pokol, G.; Ács, M.; Fogassy, E. *J. Therm. Anal.* **1994**, 42, 877. (c) Ariaans, J. A.; Bruggink, A.; Ebbers, E.; Zwanenburg, B. *Tetrahedron Asymmetry* **1998**, 9, 2745. (d) Dyer, U. C.; Henderson, D. A.; Mitchell, M. B. *Org. Process Res. Dev.* **1999**, 3, 161. (4) Smith, A. A. *Tetrahedron Asymmetry* **1998**, 9, 2925. (5) Anandamohanar P. R.; Cains P. W.; Jones A. G. *Tetrahedron Asymmetry* **2006**, 17, 1867.

(2) Jacques, J.; Collet, A.; Wilen, S. H. *Enantiomers, Racemates and Resolutions*; Wiley and Sons: New York, 1981.

**Table 1.** Initial, crystallized solid, and mother liquor composition of three crystallization experiments measured at ca. 75–83% crystallized mass recovery

exp. #	initial compositions (%)			solid composition (%)			mother liquor composition (%)		
	R,R	S,S	meso	R,R	S,S	meso	R,R	S,S	meso
GAV005-000-097-009	79.8	15.8	4.4	90	10	0	33	37	30
GAV005-000-097-010	79.8	15.8	4.4	93	7	0	36	40	24
GAV005-000-097-011	79.8	15.8	4.4	94	6	0	38	41	21

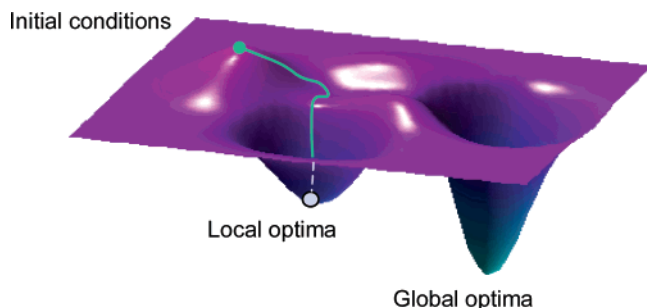


**Figure 3.** The problem of finding local optima using optimization of nonlinear functions.

The model at the centre of CRYSS is based on the algorithm discussed above. Implementation of this approach is nontrivial due to the underlying nonlinearity of the model and the possibility of finding local optima (Figure 3).

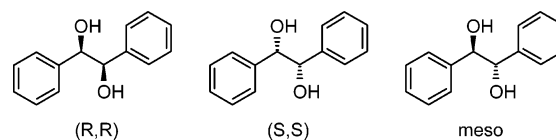
A key feature of CRYSS is that it does not require the initial separation and characterization of the individual components, nor does it require knowledge of the thermal data of the pure compounds. It has the advantage that it relies on the *actual solubility behaviour* of the components as a function of solvent volume with which it has been equilibrated and consequently is able to incorporate deviations from the ideal.

**Investigative Strategy.** The mechanistic model for multicomponent crystallizations (MultXeu) published in 1998 provides a prediction of the partitioning behaviour of components between the solid and solution phase under equilibrium conditions. No data were presented as to the applicability of this ideal model to real systems. The underlying algorithm in the CRYSS system is based on this MultXeu.

In the development of the CRYSS algorithm, extensive use was made of *simulated* crystallization data. This was generated using the MultXeu model. This type of data is perfect for the development of a robust algorithm, since one can easily generate tens of thousands of data sets, error free. In this way we were able to develop the CRYSS program, but if the underlying model was inherently incorrect, then the validity of the CRYSS approach would be somewhat flawed.

A two-phase investigative approach was selected. The first phase involves exploration of the solubility behaviour of hydrobenzoin isomers for a series of compositions in order to get first evidence of the MultXeu validity. The second phase of work demonstrates the principle of modulation of the purification profile via salt formation and extends the method to a four-component system.

**Chart 1.** Isomers of 1,2-diphenyl-1,2-ethanediol



## Results and Discussion

**Phase 1: Hydrobenzoin System.** The basic goal was to obtain the partial purification of a series of three-component hydrobenzoin blends, and from this data to make a prediction of the  $R_{\max}$  value for each blend.

This system comprises an enantiomeric (*threo*) pair and an optically inactive *meso* diastereomer (Chart 1). The binary system (of enantiomers) is well-known to crystallize as a conglomerate.<sup>6</sup> The relationship between the *threo* and the *meso* form was assumed to be conglomerate.

Equilibration with different volumes of isopropyl alcohol/water allowed the control of the relative purity and the amount of the solid which crystallized. From the measured partial purification data (Table 1) we used the CRYSS algorithm to predict three separate purification profiles. The three profiles have been overlaid on one chart (Figure 4). The mass fraction of impure solid recovered varied from 75 to 83%, but the predicted  $R_{\max}$  values all lie within 1% and are centred on 66%. Also notice that the dotted line, predicted from MultXeu, lies very close to the profiles calculated from actual measurements. The implication is that this mixture behaves nearly ideally.

In this early series of experiments, a number of other results were obtained, and in most cases complete purification of the major isomer had occurred. This was a little frustrating as it is not possible to apply the CRYSS algorithm when the crystallized solid is 100% pure. By adjusting the solvent, more partially purified samples were obtained (Table 8).

Whilst the foregoing experiments did not give us sufficient information to confirm the MultXeu model, they did alert us to the issue of the reconciliation of measured mass balance and calculated mass balance data. This bears some further explanation:

After crystallization, solid is typically isolated by filtration. On the basis of measurements made by weighing, it is possible to determine the mass fraction distributed between the solid and the solution phase at the point of phase separation.

It is slightly less obvious, but also straightforward, to calculate the same information, without recourse to weighing, by the following: (1) analysing the crystallized solid, (ii)

(6) Collet, A.; Brienne, M. J.; Jaques, J. *Chem. Rev.* **1980**, *80*, 215.

## Component Mass Fractions - Solid

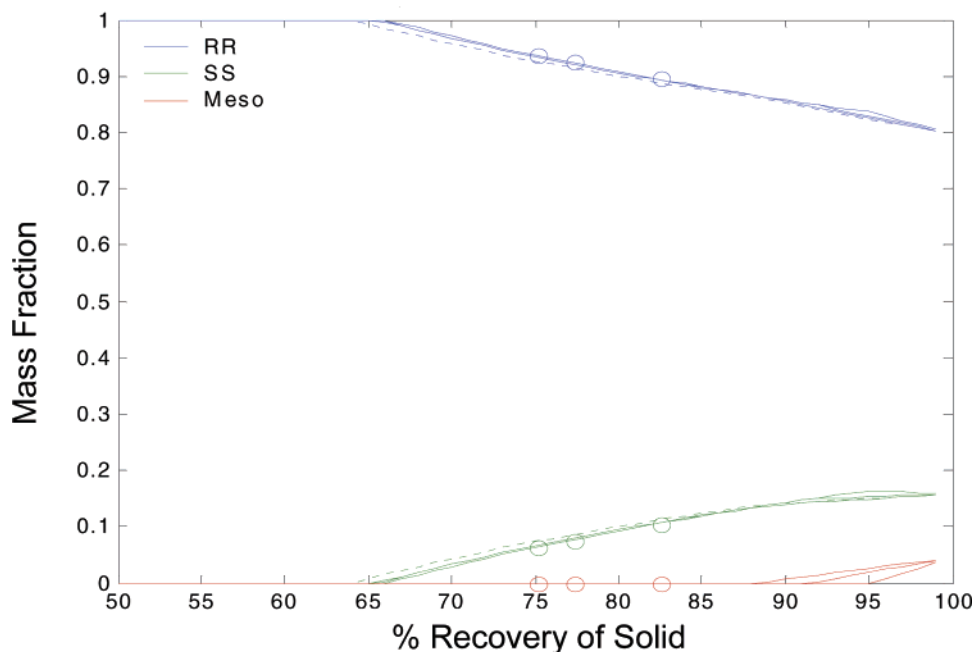


**Figure 4.** Three almost overlaying solid lines are the profiles calculated using CRYSS from the three separate experiments in Table 1; the dotted lines are based on MultXeu.

analysing the mother liquors, and (iii) knowing the composition of the initial mixture.

In Table 8 we see the data from GC analyses of the initial mixture, crystallized solid, and mother liquors, coupled with the mass data obtained by weighing the solid and mother liquor concentrate. Prior to use in the CRYSS algorithm, the compositions obtained from GC and weighing data are validated with the use of a data reconciliation algorithm.<sup>7</sup> Reconciliation is a multivariate optimization process that can make use of redundant measurements to determine how well a mass balance is satisfied in the presence of measurement errors.

Table 9 shows the results of the CRYSS algorithm. Notice that the data fall broadly into two classes, reconciled and unreconciled. We ran CRYSS three times on each data set; when the data is reconciled, it is noticeable that the prediction of a CRYSS calculation is a more consistent prediction, i.e., fewer problems with local minima (Figure 3). Additionally, we see better correlation with the “Multiple Fit  $R_{\max}$ ” value (this being obtained by fitting to all the data for each blend, reconciled or not, thereby giving a more reliable  $R_{\max}$  value). Recognize also that the variation of  $R_{\text{obs}}$  is greater than the variation of prediction of  $R_{\max}$  from the CRYSS algorithm; in principle, the  $R_{\max}$  prediction should be independent of the mass fraction of impure crystallized solid obtained.

In some entries we see material that is nearly pure, but at recoveries somewhat below the  $R_{\max}$  value. In principle this should be 100% pure. It could be (i) that imperfect separation of mother liquors has contaminated the solid or (ii) that poor control of the crystallization has led to crystal defects, which include the mother liquor.

In the case of blend 3 the results suffer from a greater spread in the single CRYSS estimates of  $R_{\max}$  (see entries 17, 18). The majority of the reconciled data has an observed recovery somewhat remote from the predicted  $R_{\max}$  value. During code development we have established that the algorithm suffers distortion the more remote the observed recovery is from the  $R_{\max}$  value, thus the greater the error in prediction of  $R_{\max}$ .<sup>8</sup> In order to get the very best prediction of  $R_{\max}$ , we used only those experiments where the data was reconciled in the CRYSS model. In Table 10 we see the  $R_{\max}$  value calculated using only this higher-quality data, alongside the prediction from MultXeu (Table 11). It is interesting that for blend 3 this “reconciled data only” prediction of 57% ties in with the transition, from impure to pure, in the range 58–56% (entries 21, 22).

We chose the hydrobenzoin system in the hope that it would behave as an ideal system. In the case of blend 2, the CRYSS  $R_{\max}$  matches the MultXeu  $R_{\max}$  value within 1%. In the other two cases, there is deviation.

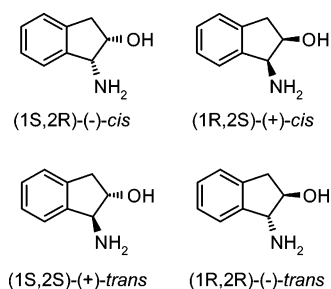
Whilst some deviation from the ideal values might be expected, it is interesting to speculate on its origin. Looking at the data (Table 10) we see that in blend 1, which contains 15% of the *meso* isomer, the CRYSS prediction has an  $R_{\max}$  of 73%, whereas the ideal approximation suggests 68%; we get a higher yield than expected. In the case of blend 3 where the mixture contains 80% *meso* isomer we see a CRYSS predicted  $R_{\max}$  of 57%, somewhat lower than the ideal prediction of 61%. Both of these observations are consistent with the *meso* isomer being more soluble than expected, based on the ideal approximation.

(7) Dempf, D.; List, T. *Comput. Chem. Eng.* **1988**, *22*, Suppl., S1023–S 1025; Madron, F. *Process Plant Performance (Measurement and Data Processing for Optimization and Retrofits)*; Ellis Horwood: New York, 1992.

(8) This discussion is beyond the scope of this publication, but it is noteworthy that substantial effort has been applied to establishing a weighting procedure for these “remote” measurements in the context of fitting multiple experiments to a single CRYSS model.

**Table 2.** Melting point and phase diagram classification for the aminoindanol series of salts

aminoindanol cmpd	mp (°C)				phase diagram type	
	cis	racemic or enantiomeric cis	trans	racemic or enantiomeric trans	cis form	trans form
aminoindanol free base	118.5	130.8	144.5	130.8	racemic cmpd	conglomerate
L-tartrate	127.1	78.2	185.8	242.1	conglomerate	conglomerate
benzoate	187.7	194.9	199.3	176.2	racemic cmpd	racemic cmpd
tosylate	195.3	183.2	212.6	215.9	racemic cmpd	racemic cmpd
acetates	151.3	144.8	160.8	137.5	racemic cmpd	racemic cmpd
phenylacetate	101.6	112.2	159.5	150.2	racemic cmpd	racemic cmpd
salicylate	142.0	158.1	170.0	186.3	racemic cmpd	racemic cmpd
mesylate	150.4	129.8	160.4	137.8	racemic cmpd	racemic cmpd
oxalate	206.6	195.5	218.6	254.6	racemic cmpd	racemic cmpd
chloride	233.9	198.2	305.9	272.6	racemic cmpd	racemic cmpd
bromide	205.9	205.9	295.1	295.1	conglomerate	conglomerate
formate	147.8	138.4	171.9	167.5	racemic cmpd	racemic cmpd

**Chart 2.** Stereoisomers of aminoindanol

In contrast to the *threo* hydrobenzoin, the *meso* isomer is unable to participate in intramolecular hydrogen bonding.<sup>9</sup> At any given moment, with an equal population of *threo* and *meso* isomers, more *meso* hydroxyl will be available for solute/solvent interactions. Other things being equal, this would result in higher *meso* isomer solubility in the isopropyl alcohol/water solvent system used above.

**Phase 2: Aminoindanol System.** Aminoindanol was selected as a suitable system for the investigation of the effect of modulation of purification by salt formation (Chart 2). The following strategy was used to guide the experimental program.

The aminoindanol stereoisomers represent a four-component system as a logical extension of the three-component hydrobenzoin system studied above.

The aminoindanol series has suitable functionality for salt formation and is expected to form crystalline products.

On the basis of our understanding developed by running many MultXeu simulations, it was anticipated that the physical properties of each salt might produce a large variation in  $R_{\max}$ .

The system is stereoisomeric and *prima facie* is expected to correlate reasonably well with the ideal approximation. This is important, since MultXeu will be used to calculate the ideal  $R_{\max}$  value. This will be compared to the  $R_{\max}$  value generated by CRYSS.<sup>10</sup>

The minor components will be present at low levels, totalling less than 10%, which may be regarded as a typical situation from organic synthesis.

Felicitous physical property interplay between the isomeric components may lead to the observation of recalcitrant impurity behaviour. In extreme situations, this might lead to one of the minor components being purified at the expense of the major component!

We required access to pure salts of all enantiomers, along with the racemic salts of the cis and trans enantiomeric pairs. Characterization by DSC allowed determination of the melting points and heats of fusion of the enantiomeric or racemic salts. Comparison of the infrared spectra of the enantiomeric and racemic salts allowed for the assignment of racemic compound, or conglomerate behaviour, for the enantiomeric pairs (Table 2).<sup>11</sup> Conglomerate behaviour is assumed for all diastereomeric relationships.<sup>12</sup>

Using the thermal data and MultXeu we calculated  $R_{\max}$  based upon a starting composition of 94, 2, 2, and 2%. This calculation was performed with a cis enantiomer and trans enantiomer present at 94%.

The  $R_{\max}$  values are presented graphically in Figure 5, and it is striking just how much the underlying physical properties of the salts affect the yield. This is the effect we want to demonstrate in the real system.

A series of crystallization experiments were performed with the aminoindanol salts. Analysis of the isolated solids was reasonable, but the situation was complicated by a number of extraneous peaks in the mother liquor analyses (probably from small amounts of oxidative decomposition). This made chromatographic determination of the composition with respect to the cis and trans enantiomers in the mother liquor problematic.

Rather than attempting to resolve the overlapping peaks in the mother liquor analysis, the approach taken was to calculate the mother liquor compositions ( $x_{L,i}$ ) from the overall (eq 2) and component (eq 3) mass balances, making

(9) Pennington, W. T.; Chakraborty, S.; Paul, I. C.; Curtin, D. Y. *J. Am. Chem. Soc.* **1988**, *110*, 6498.

(10) Determination of the actual  $R_{\max}$  value for each salt would require multiple experiments using different volumes of solvent and, hence, would multiply the body of work substantially.

(11) See Supporting Information.

(12) This could be a source of error since it is possible that in some cases *n:m* species are present; see: Prigogine, I. *Chemical Thermodynamics*; Longmans Green & Co.: London, 1954; p 374.

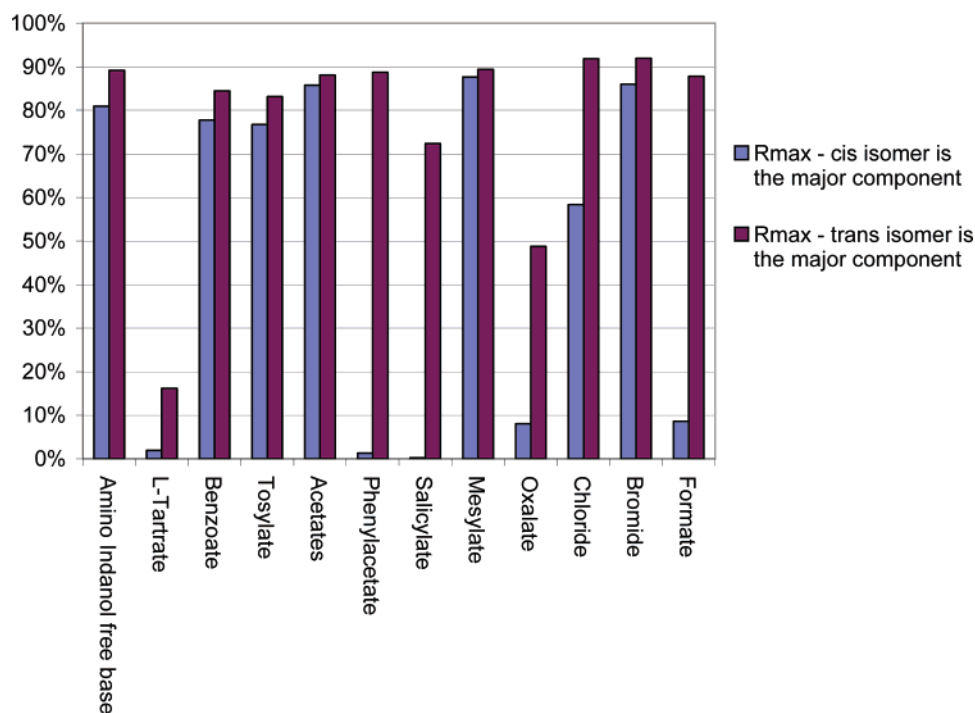


**Figure 5.** Modulation of MultXeu  $R_{\max}$  value of a mixture of aminoindanol stereoisomer salts. The composition of the mixture is 94%, 2%, 2%, 2% with either the cis enantiomer or trans enantiomer as the major isomer.

use of the initial ( $x_{0,i}$ ) and crystallized solid ( $x_{S,i}$ ) compositions for each component ( $i$ ).

$$M_0 = M_L + M_S \quad (2)$$

$$M_0 x_{0,i} = M_L x_{L,i} + M_S x_{S,i} \quad (3)$$

where  $M_0$  is the initial sample mass,  $M_S$  is the mass of crystallized solid, and  $M_L$  is the mass of compound in the mother liquor. Substituting eq 2 into (eq 3) and solving for mother liquor compositions gives:

$$x_{L,i} = \frac{M_0 x_{0,i} - M_S x_{S,i}}{M_0 - M_S} \quad (4)$$

Similarly, solving for the observed recovery ( $R_{\text{obs}}$ ) gives:

$$R_{\text{obs}} = \frac{M_S}{M_L} = \frac{x_{0,i} - x_{L,i}}{x_{S,i} - x_{L,i}} \quad (5)$$

Although expeditious, this approach removed the possibility of applying data reconciliation. The CRYSS algorithm was applied to the solubility data of the selected systems,<sup>13</sup> providing an  $R_{\max}$  prediction (Table 12). Additionally, MultXeu was used to calculate an  $R_{\max}$ , and this is plotted in Figure 6.

If the systems behave ideally and there are no experimental errors, we would expect the CRYSS  $R_{\max}$  and the MultXeu  $R_{\max}$  to have the same values. These aminoindanol salts are stereoisomeric, and thus there is some basis for near ideal behaviour; however, on the other hand some of the

enantiomeric pairs behave as racemic compounds, which is in itself a deviation from the ideal.

On first inspection of Figure 6 it seems that there is little correlation, but a more detailed inspection is very revealing. The data may be segmented into systems with good, intermediate, and poor correlation between the CRYSS and MultXeu methods.

**Systems with Good Correlation Between MultXeu and CRYSS.** There appears to be a good correlation between the MultXeu predictions and the CRYSS  $R_{\max}$  for the tartrates, tosylates, *cis*-salicylates, *trans*-bromide, *trans*-formate, and the phenylacetates (Table 3).

More detailed inspection of the purification profiles observed in these systems, indicates that in some cases the purity of the crystallized solid has improved with respect to the major isomer, concomitant with a general reduction in one or more of the minor isomers. These are the *cis*-tartrate, *cis*- and *trans*-tosylates, *trans*-bromide, *trans*-formate, and *trans*-phenylacetate. One might regard these observations as **normal purification behaviour**, where we see the major component undergoing purification in the crystallization.

Quite a different situation is observed with the *cis*-salicylates and *cis*-phenylacetate salts. Here the crystallized solids are enriched in one of the minor isomers! Inspection of the purification profile of the *cis*-salicylate series generated using MultXeu (Figure 7; with the starting composition, as in Table 3) shows that two of the three impurities are relatively easily removed, providing crystallized material of 98% purity at ~80% mass recovery. However, notice that the 1*S*,2*S*-*trans* isomer is not removed, even when greater amounts of material are partitioned into the mother liquors. Amazingly, this *trans* isomer is the component which ultimately crystallizes out at pure, albeit at very low yield,

(13) It was not possible to adequately close the mass balances for the oxalates and acetate *cis*. This was an indication that the mass measurement or analytical data for these systems contain significant errors. As such, data for these systems have not been included in the subsequent analysis.

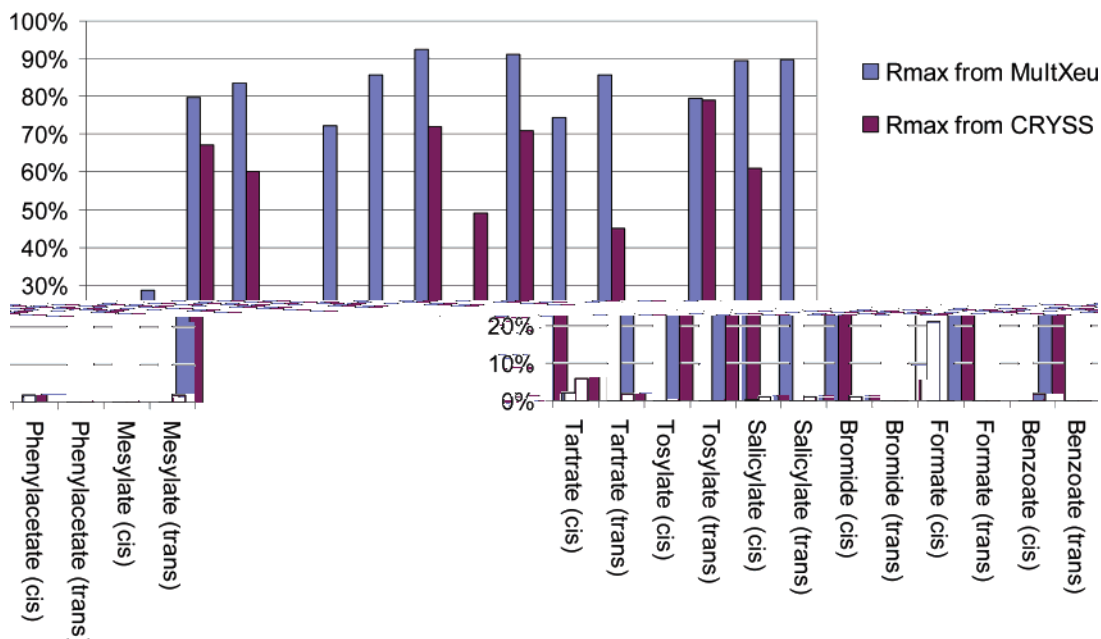


**Figure 6.** Comparison between the  $R_{\max}$  values for the mixture as calculated by the ideal approximation for that mixture, compared with that calculated by deconvolution of the solubility profile of the partially purified system using CRYSS.

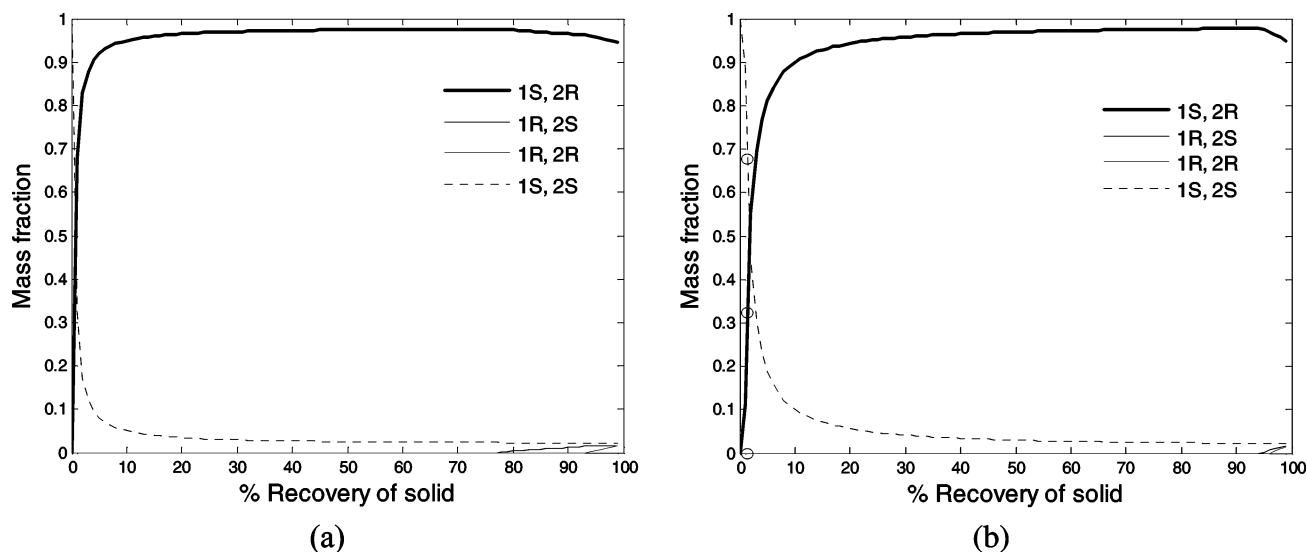


**Figure 7.** Plot of the purification profile of aminoindanol salicylate salts (cis isomer as the major component). Plot (a): ideal behaviour from MultXeu. Plot (b): model fitted to experimental data using CRYSS (unfilled circles are the experimentally observed points).

**Table 3.** Selection of Table 12 where CRYSS  $R_{\max}$  correlates well with ideal  $R_{\max}$

expt #	experiment	initial composition (%)				solid composition (%)				CRYSS $R_{\max}$ (%)	recovery ( $R_{\text{obs}}$ )(%)		MultXeu $R_{\max}$ (%)
		1S,2R	1R,2S	1R,2R	1S,2S	1S,2R	1R,2S	1R,2R	1S,2S		CRYSS		
1	<i>cis</i> -tartrate	93.5	2.2	2.2	2.0	97.9	0.5	0.6	1.1	6	17	2	
2	<i>trans</i> -tartrate	1.5	1.3	1.7	95.4	1.2	1.1	1.9	95.8	2	89	29	
3	<i>cis</i> -tosylate	94.6	1.7	2.1	1.7	99.3	0.0	0.1	0.6	67	76	80	
4	<i>trans</i> -tosylate	1.5	2.7	1.9	94.0	0.1	0.1	0.0	99.8	60	68	84	
5	<i>cis</i> -salicylate	94.3	1.7	1.9	2.1	32.3	0.0	0.0	67.7	1	1	0	
8	<i>trans</i> -bromide	1.6	2.7	1.6	94.1	0.0	0.0	0.0	99.9	72	73	93	
10	<i>trans</i> -formate	1.9	1.5	1.3	95.3	0.1	1.1	0.6	98.2	71	85	91	
15	<i>cis</i> -phenylacetate	89.6	4.2	3.7	2.5	50.3	0.0	19.8	30.0	0	1	2	
16	<i>trans</i> -phenylacetate	1.6	3.1	4.7	90.5	0.0	0.1	0.1	99.8	79	79	80	

since it was present at only 2.1% initially. Experimentally we see solid obtained at 1% recovery which shows the expected behaviour where the trans isomer is the major component.

In the *cis*-phenylacetate system, MultXeu predicts that one of the minor trans isomers is ultimately the product which is isolated pure from the crystallization. Experimentally we observe significant increase in this trans isomer in the

**Table 4.** Selection of Table 12 where CRYSS  $R_{\max}$  correlates moderately with ideal  $R_{\max}$ 

expt #	experiment	initial composition (%)				solid composition (%)				$R_{\max}$ (%)		recovery	MultXeu
		1S,2R	1R,2S	1R,2R	1S,2S	1S,2R	1R,2S	1R,2R	1S,2S	CRYSS	CRYSS	$R_{\max}$ (%)	
9	<i>cis</i> -formate	94.7	1.5	1.7	2.1	99.0	0.0	0.2	0.8	49	61	26	
12	<i>trans</i> -benzoate	1.7	1.7	94.3	2.4	0.7	0.3	97.5	1.5	45	73	86	
17	<i>cis</i> -mesylate	1.8	95.0	1.6	1.6	0.0	98.9	0.8	0.3	61	81	90	

**Table 5.** Selection of Table 12 where CRYSS  $R_{\max}$  correlates poorly with ideal  $R_{\max}$ 

expt #	experiment	initial composition (%)				solid composition (%)				$R_{\max}$ (%)		recovery	MultXeu
		1S,2R	1R,2S	1R,2R	1S,2S	1S,2R	1R,2S	1R,2R	1S,2S	CRYSS	CRYSS	$R_{\max}$ (%)	
6	<i>trans</i> -salicylate	2.2	2.0	2.0	93.8	37.5	0.0	0.0	62.5	1	2	72	
7	<i>cis</i> -bromide	94.6	1.6	1.6	2.3	91.9	0.1	3.4	4.6	1	46	86	
11	<i>cis</i> -benzoate	2.2	92.9	2.5	2.5	3.0	90.6	3.5	2.9	2	70	74	
18	<i>trans</i> -mesylate	1.9	1.9	94.1	2.0	0.1	2.4	97.5	0.1	2	77	90	

partially purified material supporting the prediction of MultXeu.

This enrichment of the minor isomer is predictable using MultXeu model, and the significance of confirming this experimentally should not be underestimated. Although we understand what is occurring in these cases, we shall refer to this as *anomalous purification behaviour*, due to the counterintuitive situation of starting with 90% pure sample which becomes less pure the more it is recrystallized!

**Systems with Intermediate Correlation between MultXeu and CRYSS.** We see in Table 4 that *cis*-formate, *trans*-benzoate, and *cis*-mesylate salts all display normal purification behaviour, but the CRYSS  $R_{\max}$  and MultXeu  $R_{\max}$  values deviate somewhat. The reason for this difference is not known, but we can speculate that there are reasons such as poorly controlled crystallization, deviations due to non-conglomerate behaviour, weighing errors, or genuine non-ideal behaviour. In the absence of data reconciliation or more substantive investigation of the purification profiles, we are unable to draw firm conclusions.

**Systems with Poor Correlation Between MultXeu and CRYSS.** In the case of the *trans*-salicylate series, the CRYSS  $R_{\max}$  is 1%, whereas MultXeu predicts an  $R_{\max}$  of 72%. We see enrichment in the minor 1S,2R-*cis* isomer.

For the *cis*-bromide series, the CRYSS  $R_{\max}$  is 1%, whereas the MultXeu predicts an  $R_{\max}$  of 86%. We see both trans isomers are enriched in the crystallized solid.

In the case of the benzoate, we see all minor isomers increasing compared with major component.

For the *trans*-mesylate, when we inspect the crystallized solid purity profile, we see the proportion of a minor *cis* isomer increasing.

We conclude that anomalous purification behaviour is occurring in all cases, and it appears that there is genuine failure of the MultXeu calculations to capture the *actual behaviour* of the systems. It is also worth noting that CRYSS has estimated the final outcome of these crystallization at observed recoveries ( $R_{\text{obs}}$ ) quite remote from the  $R_{\max}$  (see Table 5, entries 11, 18), an important feature of a predictive model.

There are fundamental reasons why discrepancies between MultXeu and CRYSS occur. Whilst we have not investigated the *actual* reason for the deviation, it is instructive to recall that the MultXeu calculation assumes conglomerate behaviour between all *cis*:*trans* relationships. Recall that we only *determined* racemic compound behaviour between enantiomeric pairs, since it is relatively straightforward by infrared analysis. This assumption could be a source of significant error in the MultXeu prediction. Formation of a 1:1 (or, in general,  $n:m$ ) complex<sup>14</sup> between a *cis* and *trans* isomer could occur and result in substantial distortion to the purification profile.

To illustrate this, we have performed MultXeu calculations for the *cis*-bromide series comparing scenarios by only changing the relationship between the minor *trans* isomers from conglomerate (Table 6) to racemic compound (Table 7). The result of this is  $R_{\max}$  falling from 86% to 28%.

The objectives of this phase of the work program were (i) to extend the CRYSS method to a four-component system, (ii) to demonstrate the modulation of  $R_{\max}$  as a function of salt formation, (iii) to test the assertion that the CRYSS  $R_{\max}$  correlates reasonably well with the MultXeu  $R_{\max}$ , and (iv) to investigate the effect of relatively low-level impurity components and possibly observe recalcitrant impurity phenomena.

Half of the systems in Table 12 correlate quite well with the ideal approximation, which is notable when we remember that CRYSS predictions are made by fitting a model to a *single experiment*. The fact that we are able to accurately predict obscure phenomena such as anomalous purification behaviour is a powerful signal that MultXeu is relevant.

Four out of the 18 systems studied displayed significant deviation between the MultXeu  $R_{\max}$  and CRYSS  $R_{\max}$  values, but this is due to unforeseen anomalous purification behaviour. These are genuine deviations from the ideal, and our experience with the *cis*-salicylate (Figure 8) and *cis*-

(14) Collet, A. In *Chiral Separations by HPLC*; Krstulovic, A.M., Ed.; Ellis Horwood: Chichester, 1989; p 97.

**Table 6.** MultXeu calculation for the *cis*-bromide series, all relationships are deemed conglomerate

recoveries	cumulative recovery = 85.70%	assume all conglomerate			
		1S,2R	1R,2S	1R,2R	1S,2S
	mp $T_i$ (°C)	205.9	205.9	295.1	295.1
	heat of fusion $\Delta H_i$ (kJ·mol <sup>-1</sup> )	19.3166	19.3166	28.5935	28.5935
	starting composition (%)	94.6	1.6	1.6	2.3
96.13	eutectic mp 132 °C, composition (%)	41.27	41.27	8.74	8.74
	composition after eutectic removal (%)	96.65		1.31	2.04
92.42	eutectic mp 167.4 °C, composition (%)	65.44		17.29	17.29
	composition after eutectic removal (%)	99.21			0.79
96.47	eutectic mp 182.2 °C, composition (%)	77.71			22.30
	composition after eutectic removal (%)	100.00			

**Table 7.** MultXeu calculation for the *cis*-bromide series, racemic compound behavior between the *trans* isomers is assumed

recoveries (%)	cumulative recovery = 28.19%	assume <i>trans</i> racemic compound			
		1S,2R	1R,2S	racemic compd	1S,2S
	mp $T_i$ (°C)	205.9	205.9	295.1	295.1
	heat of fusion $\Delta H_i$ (kJ·mol <sup>-1</sup> )	19.3166	19.3166	28.5935	28.5935
	starting composition (%)	94.6	1.6	1.6	2.3
96.44	eutectic mp 138.1 °C, composition (%)	44.93	44.93	0.25	9.91
	composition after eutectic removal (%)	96.33		1.65	2.02
90.80	eutectic mp 181.3 °C, composition (%)	76.86		1.22	21.93
	composition after eutectic removal (%)	98.31		1.69	
32.19	eutectic mp 203.4 °C, composition (%)	97.51		2.50	
	composition after eutectic removal (%)	100.00			

**Table 8.** Analytical data from EJRO22/006/012/1

exp. #	blend	$x_0$ (%)			$x_L$ (%)			$x_S$ (%)			recovery ( $R_{obs}$ ) (%) (CRYSS)	reconciled	$M_S$ (mg/mg) (%)	$M_L$ (mg/mg) (%)	$M_S$ from $M_L$ (mg/mg) (%)
		R,R	S,S	<i>meso</i>	R,R	S,S	<i>meso</i>	R,R	S,S	<i>meso</i>					
1	1	5.0	79.9	15.1	20.3	24.1	55.5	2.6	86.3	11.1	90	1	89	6	94
2	1	5.0	79.9	15.1	22.8	23.9	53.4	1.8	88.6	9.6	87	1	87	10	90
3	1	5.0	79.9	15.1	23.6	24.4	52.1	0.8	89.9	9.3	85	1	84	13	87
4	1	5.0	79.9	15.1	23.6	24.9	51.5		94.1	5.9	80	1	81	17	83
5	1	5.0	79.9	15.1	12.2	44.6	43.2		99.4	0.6	65		68	31	69
6	1	5.0	79.9	15.1	10.7	50.9	38.4	0.2	98.9	0.9	61		64	34	66
7	1	5.0	79.9	15.1	9.5	57.3	33.2		99.6	0.4	54		61	38	62
8	1	5.0	79.9	15.1	9.0	60.5	30.5		99.5	0.5	50		56	42	58
9	2	79.9	15.1	5.1	21.8	23.7	54.5	84.9	14.3	0.9	92	1	91	7	93
10	2	79.9	15.1	5.1	24.5	25.4	50.1	86.8	13.2		89		86	9	91
11	2	79.9	15.1	5.1	28.9	29.7	41.4	87.1	12.9		88	1	87	11	89
12	2	79.9	15.1	5.1	32.0	33.1	34.9	88.1	11.9		85	1	85	12	88
13	2	79.9	15.1	5.1	41.9	44.4	13.7	99.2	0.8		67	1	67	26	74
14	2	79.9	15.1	5.1	48.8	40.1	11.2	99.6	0.4		62		64	30	70
15	2	79.9	15.1	5.1	52.6	36.4	11.0	99.7	0.3		58	1	60	39	61
16	2	79.9	15.1	5.1	56.6	33.3	10.0	99.7	0.3		55	1	56	43	57
17	3	4.9	15.0	80.0	23.4	23.5	53.1	3.0	14.9	82.1	92	1	91	7	93
18	3	4.9	15.0	80.0	24.3	24.5	51.3	2.6	12.8	84.6	87	1	89	10	90
19	3	4.9	15.0	80.0	25.1	25.1	49.8	0.6	11.2	88.1	80		85	14	86
20	3	4.9	15.0	80.0	24.0	25.8	50.2	0.2	10.6	89.3	77		81	18	82
21	3	4.9	15.0	80.0	12.0	35.0	53.1	0.1	0.5	99.4	58	1	60	37	63
22	3	4.9	15.0	80.0	10.1	34.4	55.5			100.0	56		59	41	59
23	3	4.9	15.0	80.0	9.7	28.7	61.7			100.0	48		53	47	53
24	3	4.9	15.0	80.0	10.3	26.6	63.1			100.0	45		50	47	53

<sup>a</sup> The initial composition ( $x_0$ ), mother liquor composition ( $x_L$ ), and the crystallized solid composition ( $x_S$ ) are presented. The mass balance from the composition data alone has been compared with the measured mass data, and data sets that are deemed to reconcile have been flagged with a 1.

phenylacetate salts tends to support the CRYSS prediction of massive yield erosion in these systems.

## Conclusions

We have investigated the purification profile of the hydrobenzoin system in some detail and found that the data support the ideal mechanistic model (MultXeu) on which the CRYSS approach is based.<sup>15</sup>

We have seen that, as long as the analytical data are of sufficient quality, a single measurement somewhere along

the purification profile can be used to calculate the maximum yield of pure component from an optimized crystallization. It is noted, however, that such a prediction in any isolated system may be subject to error for a variety of reasons. Some of these may be intrinsic phenomena, only realized close to the point of purification (i.e., terminal solid solution), or may be due to error introduced through measurement, poorly

(15) That purification, under equilibrium conditions, can be calculated in a series of discrete stages, and using a mechanistic model within an optimizer can be used to deconvolute the solubility behaviour.

**Table 9.** CRYSS Calculation on the Data Set of Table 8

exp. #	blend	$x_0$ (%)			$x_L$ (%)			$x_S$ (%)			recovery ( $R_{obs}$ ) (%)	$R_{max}$ (%)	$R_{max}$ (%)	$R_{max}$ (%)	$R_{max}$ (%)	rec'ld
		R,R	S,S	meso	R,R	S,S	meso	R,R	S,S	meso	(CRYSS)	multiple fit (CRYSS) <sup>a</sup>	single CRYSS est.	single CRYSS est.	single CRYSS est.	
1	1	5.0	79.9	15.1	20.3	24.1	55.5	2.6	86.3	11.1	90		73	73	79	1
2	1	5.0	79.9	15.1	22.8	23.9	53.4	1.8	88.6	9.6	87		73	73	73	1
3	1	5.0	79.9	15.1	23.6	24.4	52.1	0.8	89.9	9.3	85		72	74	73	1
4	1	5.0	79.9	15.1	23.6	24.9	51.5		94.1	5.9	80		73	73	72	1
5	1	5.0	79.9	15.1	12.2	44.6	43.2		99.4	0.6	65	73	79	80	63	
6	1	5.0	79.9	15.1	10.7	50.9	38.4	0.2	98.9	0.9	61		58	57	76	
7	1	5.0	79.9	15.1	9.5	57.3	33.2		99.6	0.4	54		51	80	73	
8	1	5.0	79.9	15.1	9.0	60.5	30.5		99.5	0.5	50		50	80	80	
9	2	79.9	15.1	5.1	21.8	23.7	54.5	84.9	14.3	0.9	92		66	65	65	1
10	2	79.9	15.1	5.1	24.5	25.4	50.1	86.8	13.2		89		66	65	66	
11	2	79.9	15.1	5.1	28.9	29.7	41.4	87.1	12.9		88		65	65	65	1
12	2	79.9	15.1	5.1	32.0	33.1	34.9	88.1	11.9		85		65	65	65	1
13	2	79.9	15.1	5.1	41.9	44.4	13.7	99.2	0.8		67	66	66	66	66	1
14	2	79.9	15.1	5.1	48.8	40.1	11.2	99.6	0.4		62		60	73	75	
15	2	79.9	15.1	5.1	52.6	36.4	11.0	99.7	0.3		58		74	64	58	1
16	2	79.9	15.1	5.1	56.6	33.3	10.0	99.7	0.3		55		79	63	61	1
17	3	4.9	15.0	80.0	23.4	23.5	53.1	3.0	14.9	82.1	92		47	47	46	1
18	3	4.9	15.0	80.0	24.3	24.5	51.3	2.6	12.8	84.6	87		49	49	49	1
19	3	4.9	15.0	80.0	25.1	25.1	49.8	0.6	11.2	88.1	80		52	51	51	
20	3	4.9	15.0	80.0	24.0	25.8	50.2	0.2	10.6	89.3	77		52	57	54	
21	3	4.9	15.0	80.0	12.0	35.0	53.1	0.1	0.5	99.4	58	55	57	57	70	1
22	3	4.9	15.0	80.0	10.1	34.4	55.5			100.0	56					
23	3	4.9	15.0	80.0	9.7	28.7	61.7			100.0	48					
24	3	4.9	15.0	80.0	10.3	26.6	63.1			100.0	45					

<sup>a</sup> There are two types of CRYSS calculation in this table: single CRYSS estimates, where the whole purification profile is calculated on the basis of a single experiment (note CRYSS has been run on the data three times), and multiple fit where all of the data for a particular blend is used. Where the crystallized solid is 100% pure, it is impossible to make a meaningful CRYSS prediction (however, these are useable data when fitting CRYSS to multiple experiments).

**Table 10.** CRYSS calculation on the data set of Table 8 using only data which reconcile each blend (1–3)

exp. #	blend	initial composition ( $x_0$ ) (%)			recovery ( $R_{obs}$ ) (%)	multiple fit yield <sup>a</sup> (%)	reconciled	ideal $R_{max}$ (%)
		R,R	S,S	meso	(CRYSS)	$R_{max}$		
1	1	5.0	79.9	15.1	90		1	
2	1	5.0	79.9	15.1	87		1	
3	1	5.0	79.9	15.1	85	73	1	68
4	1	5.0	79.9	15.1	80		1	
9	2	79.9	15.1	5.1	92		1	
11	2	79.9	15.1	5.1	88		1	
12	2	79.9	15.1	5.1	85		1	
13	2	79.9	15.1	5.1	67	66	1	65
15	2	79.9	15.1	5.1	58		1	
16	2	79.9	15.1	5.1	55		1	
17	3	4.9	15.0	80.0	92		1	
18	3	4.9	15.0	80.0	87	57	1	61
21	3	4.9	15.0	80.0	58		1	

<sup>a</sup> The  $R_{max}$  values are for fitting all of the data for each blend to one CRYSS model and represent the best possible predictions for  $R_{max}$ . These values should be compared with the prediction in Table 9. Note entries corresponding to 17 and 18, where deviation in single CRYSS prediction varies from the multiple fit results. This behaviour is observed when the prediction is made at mass fractions remote from the  $R_{max}$  value. Note that the deviation from ideality is explained by increased solubility of the *meso* isomer above that expected from the ideal approximation.

controlled crystallization, or difficulties of separation. This implies that a robust operational and analytical protocol is required for running crystallization experiments.

During the course of the hydrobenzoin study, there has been some discussion on fitting the data from multiple experiments. Whilst the focus of this study is to prove the underlying theory of the approach, in principle requiring only a single measurement, the approach is far more powerful if

the data from experiments at a range of mass recoveries are consolidated in one model.

We saw that, although certain hydrobenzoin mixtures deviate from the ideal prediction, the performance of that system within CRYSS was consistent. This accommodation of deviation from the ideal is an important feature which has the potential to allow the extension of the method to non-isomeric components and provides an opportunity to

**Table 11.** Calculation of the three hydrobenzoin blends using the ideal approximation

		blend 1			
A	recoveries	cumulative recovery = 67.83%	RR	SS	meso
		mp $T_i$ (°C)	150	150	139
		heat of fusion $\Delta H_i$ (kJ·mol <sup>-1</sup> )	33.6450	33.6450	35.1950
		starting composition (%)	5	80	15
	83.68%	eutectic mp: 103.7 °C, composition (%)	30.89	30.89	38.23
		composition after eutectic removal (%)		89.45	10.55
	81.06%	eutectic mp: 116.8 °C, composition (%)		44.29	55.72
		composition after eutectic removal (%)		100.00	
		blend 2			
B	recoveries	cumulative recovery = 64.83%	RR	SS	meso
		mp $T_i$ (°C)	150	150	139
		heat of fusion $\Delta H_i$ (kJ·mol <sup>-1</sup> )	33.6450	33.6450	35.1950
		starting composition (%)	80	15	5
	86.77%	eutectic mp 103.7 °C, composition (%)	30.89	30.89	38.23
		composition after eutectic removal (%)	87.36	12.64	
	74.72%	eutectic mp 121.4 °C, composition (%)	50.00	50.00	
		composition after eutectic removal (%)	100.00		
		blend 3			
C	recoveries	cumulative recovery = 61.20%	RR	SS	meso
		mp ( $T_i$ )/°C	150	150	139
		heat of fusion ( $\Delta H_i$ )/kJ·mol <sup>-1</sup>	33.6450	33.6450	35.1950
		starting composition (%)	4.9	15.0	80.0
	84.03%	eutectic mp 103.7 °C, composition (%)	30.89	30.89	38.23
		composition after eutectic removal (%)		12.03	87.97
	72.83%	eutectic mp 116.8 °C, composition (%)		44.29	55.72
		composition after eutectic removal (%)			100.00

extend the approach to include solvent descriptor data via multivariate techniques.<sup>16</sup>

We extended the CRYSS method to a four-component system and showed modulation of the purification profile by salt formation. We saw quite reasonable correlation between the ideal approximation and, in most cases where substantial deviations were observed, were able to conclude that the deviations were due to unexpected anomalous purification behaviour rather than experimental error or poorly controlled crystallizations.

Taking the information presented as a whole, we have a body of evidence which confirms the MultXeu model in that it accurately describes systems which behave nearly ideally.

In order to develop the CRYSS algorithm, extensive testing using large amounts of simulated data was conducted. Consequently, we were confident that the numerical aspects of the approach were on firm ground. However, confirmation of the MultXeu theory and the application of CRYSS to real data is of course central to gaining more widespread acceptance of the approach.

## Experimental Section

All solvents and reagents were obtained from commercial sources. Each hydrobenzoin enantiomer was synthesised

according to the method outlined by Sharpless et al.<sup>17</sup> and recrystallized from hot acetone solution. The recrystallization procedure was repeated twofold, with a combined overall recovery of 85%. Purity of the obtained materials was assessed by means of gas chromatography (Chirasil-DEX CB column 25 m × 0.25 mm, 0.25 μm film width, split/splitless with a split ratio of 20 at an injector temperature of 200 °C, carrier He at 5 mL/min, isothermal program at an oven temperature of 180 °C, FID detector at 200 °C), in all cases resulting in a purity of greater than 99.8% by area. (1*S*,2*S*)-aminoindanol was prepared as described by Hu et al.<sup>18</sup> Purification of the crude *trans*-aminoindanol mixture was achieved by recrystallization of the (conglomerate) hydrobromide salt from hot methanolic solution. The recrystallization procedure was repeated three times, with a combined overall recovery of 90%. Again, the purity of the materials was assessed by means of gas chromatography (Chirasil-DEX CB column 25 m × 0.25 mm, 0.25 μm film width, split/splitless with a split ratio of 20 at an injector × temperature of 200 °C, carrier He at 3.5 mL/min, temperature program 145 °C (1 min)—ramp 2 °C/min (10 min)—165 °C (1 min), FID detector at 200 °C), again in all cases, resulting in a purity greater than 99.8% by area. The reported

(16) McKay, B.; Hoogenraad, M.; Damen, E. W. P.; Smith, A. A. *Curr. Opin. Drug Discovery Dev.* **2003**, *6*, 966.

(17) Sharpless, K. B.; Amberg, W.; Bennani, Y. L.; Crispino, G. A.; Hartung, J.; Jeong, K.-S.; Wong, H.-L.; Morikawa, K.; Wang, Z.; M.; Xu, D.; Zhang, X. L. *J. Org. Chem.* **1992**, *57*, 2768.

(18) Hu, H.; Hollinshead, S. P.; Hall, S. E.; Kalter, K.; Ballas, L. M. *Bioorg. Med. Chem. Lett.* **1996**, *6*, 973.

**Table 12.** Comparison between  $R_{\max}$  calculated from the ideal approximation and predicted by CRYSS on the basis of the purity profiles of partially purified systems

exp. #	salt type (major isomer)	initial composition (%)				liquor composition (%)				solid composition (%)				$R_{\max}$	recovery ( $R_{\text{obs}}$ )(%)	ideal (%)
		1S,2R	1R,2S	1R,2R	1S,2S	1S,2R	1R,2S	1R,2R	1S,2S	1S,2R	1R,2S	1R,2R	1S,2S	CRYSS	CRYSS	$R_{\max}$
1	tartrate (cis)	93.5	2.2	2.2	2.0	92.7	2.6	2.6	2.2	97.9	0.5	0.6	1.10	6	17	2
2	tartrate (trans)	1.5	1.3	1.7	95.4	4.1	3.3	0.0	92.6	1.2	1.1	1.9	95.80	2	89	29
3	tosylate (cis)	94.6	1.7	2.1	1.7	79.5	7.0	8.4	5.1	99.3	0.0	0.1	0.60	67	76	80
4	tosylate (trans)	1.5	2.7	1.9	94.0	4.4	8.1	5.8	81.7	0.1	0.1	0.0	99.80	60	68	84
5	salicylate (cis)	94.3	1.7	1.9	2.1	95.1	1.7	1.9	1.2	32.3	0.0	0.0	67.70	1	1	0
6	salicylate (trans)	2.2	2.0	2.0	93.8	1.6	2.0	2.0	94.4	37.5	0.0	0.0	62.50	1	2	72
7	bromide (cis)	94.6	1.6	1.6	2.3	96.8	2.9	0.0	0.3	91.9	0.1	3.4	4.60	1	46	86
8	bromide (trans)	1.6	2.7	1.6	94.1	5.9	9.6	6.0	78.5	0.0	0.0	0.0	99.90	72	73	93
9	formate (cis)	94.7	1.5	1.7	2.1	87.8	3.9	4.1	4.2	99.0	0.0	0.2	0.80	49	61	21
10	formate (trans)	1.9	1.5	1.3	95.3	12.3	3.6	5.3	78.8	0.1	1.1	0.6	98.20	71	85	91
11	benzoate (cis)	2.2	92.9	2.5	2.5	0.3	98.2	0.1	1.4	3.0	90.6	3.5	2.90	2	70	74
12	benzoate (trans)	1.7	1.7	94.3	2.4	4.2	5.3	85.8	4.6	0.7	0.3	97.5	1.50	45	73	86
15	phenylacetate (cis)	89.6	4.2	3.7	2.5	89.9	4.3	3.5	2.3	50.3	0.0	19.8	30.00	0	1	2
16	phenylacetate (trans)	1.6	3.1	4.7	90.5	7.7	14.4	22.2	55.7	0.0	0.1	0.1	99.80	79	79	80
17	mesylate (cis)	1.8	95.0	1.6	1.6	9.4	78.6	4.9	7.1	0.0	98.9	0.8	0.30	61	81	90
18	mesylate (trans)	1.9	1.9	94.1	2.0	8.3	0.3	82.6	8.8	0.1	2.4	97.5	0.10	2	77	90

chromatography methods were used for all other analysis discussed here.

**Experimental Protocol for the Crystallization of a Mixture of Hydrobenzoin from a Water/Isopropanol Mixture.** The blends of hydrobenzoin isomers were weighed manually into agate mortar and ground gently. The resulting blends were homogenized on a roller bank over a period of 24 h in order to achieve homogeneous composition. For each blend the appropriate amounts of solid were distributed into the reactors, after which an amount of isopropanol/water mixture was added. The reactors were placed in to a H+P 24.25 reactor block equipped with a Huber 390W HT thermostat. The reactors were subjected to the following thermo cycle: heat to 80 °C with 5 °C/min, hold for 15 min, cool to 20 °C with 5 °C/min. This cycle was repeated three times. After this, a fast heat-slow cool cycle was performed (cool ramp of 1 °C/min) to achieve crystallization at a final temperature of 10 °C at which temperature an aging time of 16 h was applied. After settling, the solids were isolated by means of vacuum filtration (400 mbar) over 10  $\mu\text{m}$  filters. The filter cakes were washed with 3 aliquots of cold water/isopropanol mixture of the appropriate composition. The mother liquors and the isolated solids (after drying in vacuo to constant weight) were analyzed by GC (see method above).

**Experimental Protocol for the Crystallization of Aminoindanol Salts from a Mixture of 1,2-Dichloroethane and Tetrahydrofuran.** The compositions were weighed manually into a 1.8 mL HPLC vial. For each isomeric blend 1500  $\mu\text{L}$  of a 2:1 mixture by volume of 1,2-dichloroethane and tetrahydrofuran was added. The reactors were placed in

to an Avantium Technologies Crystal16 reactor system. The reactors were subjected to the following thermo cycle: heat to 67 °C with 5 °C/min, hold for 15 min, cool to 20 °C with 5 °C/min. This cycle was repeated three times to ensure equilibrium. After this, a fast heat/slow cool cycle was performed (cool ramp of 1 °C/min) to achieve crystallization at 7 °C at which temperature an aging time of 24 h was applied. After settling, the solids were isolated by means of vacuum filtration (200 mbar) over 10  $\mu\text{m}$  filters. The filter cakes were washed with 3 aliquots of cold tetrahydrofuran. The mother liquors and the isolated solids (after drying in vacuo to constant weight) were analyzed by GC after derivatization using trifluoroacetic anhydride.

#### Acknowledgment

We thank Lisa Agocs, François Gilardoni, and Darren Rhodes.

#### Supporting Information Available

(i) DSC ( $\text{mp}/\Delta H_{\text{fusion}}$ ) data for the aminoindanol salt series, (ii) IR traces of various aminoindanol salts (ent. & rac.), (iii) results of ideal approximation (MultXeu) calculations for aminoindanol salts Supporting Information Figure 5, (iv) results of ideal approximation (MultXeu) calculations for aminoindanol salts Supporting Information Figure 6. This material is available free of charge via the Internet at <http://pubs.acs.org>

Received for review July 31, 2006.

OP060153S